



Influence of propeller fouling on propulsion performance of an actual ship: a long-term analysis focusing on the power for keeping propeller's rotation of a controllable pitch propeller

Hiroaki Torii^{1,2} · Hiroyasu Kifune¹

Received: 12 February 2023 / Accepted: 8 October 2023 / Published online: 28 October 2023
© The Author(s) 2023, corrected publication 2024

Abstract

This study focuses on the shaft power at the neutral angle of a controllable pitch propeller to analyze the change in the required power due to propeller fouling. It is named and defined as a power for keeping propeller's rotation (RP) because a propeller does not generate the net thrust to push the hull but dissipates the power to keep its constant speed. Statistical analysis was conducted using a decade of the observed data from a research vessel. This study assumed that the change in RP can be considered as an indicator showing the state of propeller fouling. In addition, the state of fouling on the hull can be estimated indirectly based on RP because the data correlated the shaft power under several operating conditions with RP on the same voyage. The fouling state was classified into three conditions based on RP. The comparison of shaft power at the same ship speed between the clean condition and the serious fouled condition showed that the shaft power was increased by 35% on average due to fouling. When the ship navigates under 10 knots, propeller fouling has a larger impact on the increase in shaft power than hull fouling.

Keywords Propellers · Biofouling · Monitoring data · Ship propulsion · Shaft power

1 Introduction

Biofouling has a significant impact on the propulsion efficiency of all vessels. It is the build-up of microorganisms, plants, algae, or small animals on the surface of the hull and the propeller. Biofouling increases the surface roughness of the hull and the propeller, which leads to an increase in the frictional resistance. Consequently, an increase in resistance causes the required shaft power to be increased to maintain a constant ship speed, or ship speed is decreased at a constant power [1]. These factors affect fuel consumption and GHG emissions [2]. According to a report that summarizes

studies on fouling on a hull [3], biofouling as thin as 0.5 mm covering up to 50% of a hull surface can trigger an increase in GHG emissions in the range of 20–25%. For more severe biofouling conditions, GHG emissions can be increased by up to 55%.

In addition, some studies indicate that biofouling causes the issue of Invasive Aquatic Species (IAS) [4]. Some aquatic species attaching to a vessel are transported by ships to non-indigenous habitats and seriously affect ecosystems. IAS are considered one of the greatest threats to marine ecosystems [5]. To control biofouling, almost all vessels have an antifouling (AF) paint coating over their underwater hull [1, 6]. However, AF paint cannot completely prevent the marine organisms on a ship. Thus, biofouling has become a serious problem for GHG emissions and protection of the marine environment.

International Maritime Organization (IMO) adopted Chapter 4 of MARPOL Annex VI in 2013, which established Ship Energy Efficiency Management Plan (SEEMP) and called for substantial improvements in propulsion efficiency [7, 8]. In the Guidelines of SEEMP [9], hull maintenance is referred to as one of the practices for the fuel-efficient operation of ships. This guideline states that docking

✉ Hiroaki Torii
hiro.torii23122b@gmail.com;
hiroaki_torii@monohakobi.com

Hiroyasu Kifune
kifune@kaiyodai.ac.jp

¹ Department of Marine Electronics and Mechanical Engineering, Tokyo University of Marine Science and of Technology, Etchujima, Koto, Tokyo 1358533, Japan

² Present Address: Maritime & Logistics Technology Group, MTI Co., Ltd., Chiyoda, Tokyo 1000005, Japan

intervals should be integrated with ship operators' ongoing assessment of ship performance. SEEMP also suggests that propeller cleaning and polishing or even an appropriate coating may significantly increase fuel efficiency, and the need for ships to maintain efficiency through in-water hull cleaning should be recognized and facilitated by port states. The purpose of these maintenance works on the hull and the propeller is to remove biofouling and reduce the negative influence of fouling on propulsive performance. To approach the issue of biofouling, the Glofouling Partnerships Project was initiated by IMO, United Nations Development Programme (UNDP), and Global Environment Facility (GEF) in December 2018. Hull cleaning and propeller polishing are recommended to control biofouling appropriately [3].

Biofouling had been recognized as having a negative impact on propulsion performance since the early 20th century. Several experimental and numerical methods that predict the fouling influence had been developed in many studies [10–14]. Some studies have investigated the influence of hull fouling [10–13] and propeller fouling [14] based on model-scale experiments. However, few studies have applied the results of model-scale experiments to fouling on an actual ship because the surface roughness increased by biofouling cannot be scaled up or down [15].

Since the 1950s, the influence of fouling has been predicted using the boundary layer similarity law [16–18]. This similarity law can predict the influence of full-scale roughness on an arbitrary length of a body with the same roughness. Reference [18] attempted to predict the fouling influence using the boundary layer similarity law. This research confirmed good agreement between the simulated result based on the model-scale experiment and the result of a sea trial on an actual ship. In addition, the influence of fouling in several fouling situations was estimated in the simulation. However, this method can only calculate the influence of a given roughness on the frictional resistance of a flat plate of a ship length. Demirel [19] argued that it is still worth investigating the phenomenon by means of a fully nonlinear method, such as Computational Fluid Dynamics (CFD), to study how the roughness caused by biofouling affects the resistance of the ship in detail.

Since the performance of computers has improved, the influence of fouling on full-scale models has been estimated using CFD. In studies using CFD, the fouling influence was simulated by changing the representative roughness heights of the hull and propeller. Several studies focusing on the hull fouling have been conducted, for example, by Demirel [19], Song [20, 21], and Farkas [22, 23]. Furthermore, the influence of propeller fouling was studied by Song [15].

Reference [24] approached the issue of how self-propulsion characteristics are affected by the fouling in four scenarios: 1. Clean hull and fouled propeller; 2. Fouled hull and clean propeller; 3. Both hull and propeller are clean; 4. Both

two are fouled. The simulation was applied to over 200 m long container ship which goes on 24 knots. The simulation results showed that the fouling has a stronger impact on the hull than on the propeller in terms of the required power to maintain constant ship speed. However, these studies still have significant challenges that need to be evaluated using actual ship data.

On the other hand, several studies have investigated the fouling influence on an actual ship. As the old study, the towing experiment of the ex-destroyer *Yudachi* was conducted to examine the influence of hull fouling by Izubuchi [10, 11, 25] in 1934. 1st-class destroyer *Sagiri* towed *Yudachi* which was moored for a year to grasp the relevance between ship speed and resistance. The experiment showed that the resistance of the ship was increased approximately twice. Recently, onboard monitoring systems that measure ship performance have been developed, and some studies have analyzed the influence of fouling on ship performance based on onboard monitoring data [26–29]. However, no study has evaluated the influence of fouling by separating the propeller and hull based on actual ship data. It was not possible to figure only the biofouling influence of the propeller from the observed data because the ship performance was affected by both hull roughness and propeller roughness.

This study evaluates the influence of biofouling on the propeller by analyzing the observed big data recorded in an actual research vessel for 10 years. The ship that this study focused on had controllable pitch propeller (CPP) as its main propeller. By investigating the propeller's operation, the influence of biofouling on the propeller was extracted when it operated in a specific condition that it did not provide any thrust force by tuning its blade angle in neutral. Through the analysis using long-term observations, the influence of the propeller fouling on the required shaft power was clarified.

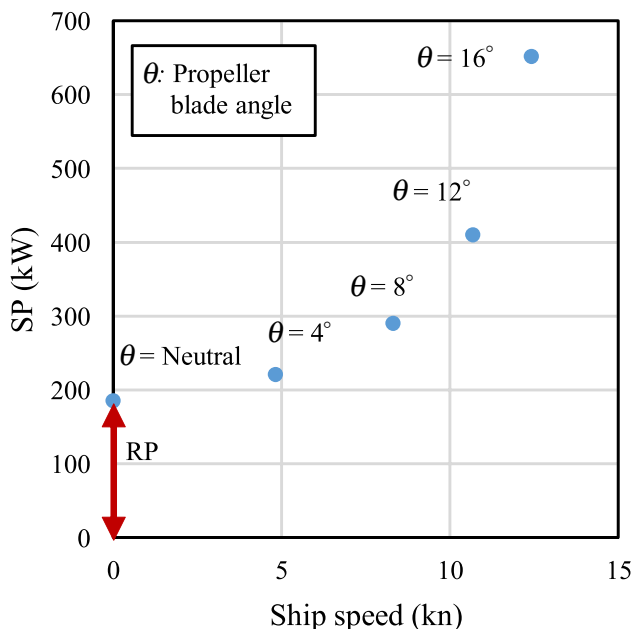
Second, the change in propulsion performance affected by fouling is analyzed during ship navigation in Chapter 4. Finally, comparing the results of Chapters 3 and 4, the influence of propeller on the total power change by biofouling is evaluated in Chapter 5.

2 Monitoring data of the ship performance

The data this paper focuses on were observed from 2011 to 2020 on the research vessel “ship A”. Ship A used to navigate Tokyo Bay. A middle-speed diesel engine and 4-blade CPP were equipped to provide propulsion power. Table 1 lists the specifications of ship A. The ship data were obtained using an onboard monitoring system. The observed data including ship speed, shaft power, shaft speed, propeller blade angle, rudder angle, heading course, true wind speed, and true wind direction were observed and recorded every second. Specifically, the log speed was measured by

Table 1 Specifications of ship A

Items	Specification
Length over all	49.9 m
Shaft speed	300 min ⁻¹
Rated power of the main engine	1000 kW
Maximum ship speed at sea trial	14.5 kn
Propeller	4-blade CPP

**Fig. 1** Relation between SP, ship speed, and blade angle of a CPP

an electromagnetic (EM) log sensor, and the shaft power was obtained using a torque sensor equipped with the intermediate shaft.

3 Power for keeping propeller's rotation (RP)

3.1 Definition of RP

To observe the influence of propeller fouling, this study focuses on the shaft power under a specific condition in which CPP does not provide any net thrust force to push the hull while it is driven at the rated speed of 300 min⁻¹. Generally, CPP is driven at the rated speed, and its blade angle is changed to control the thrust force. Fig. 1 shows the relationship between the shaft power (SP) and blade angle θ on CPP. These data were observed in the steady state. As is clear from the figure, the propeller requires the power to some extent for keeping its constant speed,

even if its blade angle is neutral. This power is not used effectively, and is dissipated only. The root cause of this power loss can be attributed to several main factors [30]. For instance, the frictional resistance of the blades, power loss due to stirring sea water, and accelerating loss to push the water forward and backward, although no net thrust force is generated. This power loss is defined as the power for keeping propeller's rotation (RP) in this paper.

Song [15] conducted a simulation to analyze how fouling on the propeller affects its characteristics in two components: the pressure component and shear (frictional) component. The simulation shows that the pressure torque component is decreased slightly when the surface fouling of the propeller is increased. On the other hand, the frictional torque component is raised significantly. As a result, the required power to maintain its speed increases when the propeller is fouled. In the case of an actual ship, the propeller torque is related to the hull condition, because the propeller generates a force to push the hull. However, RP values are not influenced by the hull resistance and ship speed because the propeller does not consume power to push the hull while it runs in a neutral angle. Needless to say, fouling of the hull does not influence RP values. Hence, it is assumed that the increase in RP indicates that the propeller fouling is proceeding. By analyzing RP, it is expected to illustrate how fouling affects frictional loss of the propeller.

3.2 Method to obtain RP value from observed data

The RP values were extracted from the observed data just before the start of navigation. Fig. 2 shows a sample of the observed main engine speed, shaft speed, CPP blade angle, rudder angle, shaft power, and ship speed. Before starting the voyage, the main engine runs under the idling condition for a while so that engineers check all operating statuses in the propulsion system and the power plant. In this figure, the operation can be classified into three periods as follows:

- (1) The main engine is running, but the shaft is not rotating because the clutch is not engaged;
- (2) The main engine drives the shaft and the propeller; however, the net thrust force is not provided because the propeller blade angle θ is neutral;
- (3) The propeller blade angle goes up, and the ship starts its navigation.

In the second period, SP is not converted into the thrust force at all. RP is determined by averaging the value of SP in the second period. Hence, RP was obtained from the data that satisfied the following criteria.

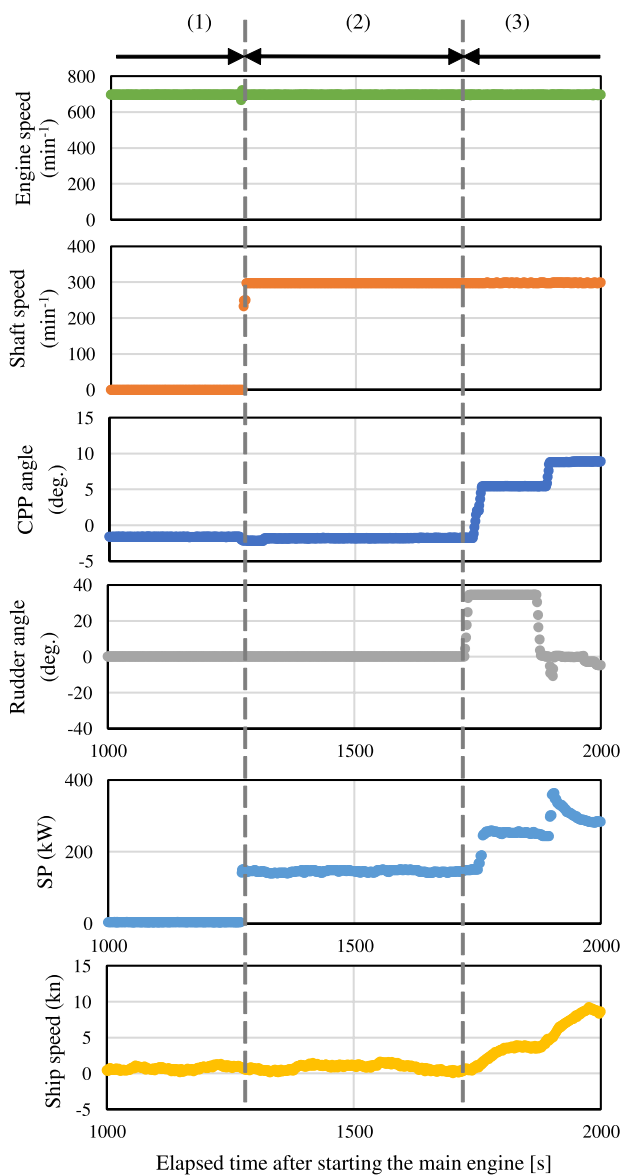


Fig. 2 Measuring period of RP before starting navigation

- (a) Shaft speed is over 290 min^{-1} . The data with shaft speed under 290 min^{-1} were filtered to exclude the transient data from low to the rated speed.
- (b) Propeller blade angle is between -2.5 and -1.0 deg. The neutral blade angle of the propeller varies for each vessel. The neutral angle of the propeller is approximately -1.8 deg. for ship A. In the second period, the value of blade angle has some variation because seafarers tune it manually. However, judging from the long-term observation, there was no big difference in SP in the range of -2.5 and -1.0 deg.
- (c) Rudder angle is under ± 1.0 deg. The rudder angle may affect the current flow around the propeller, which may

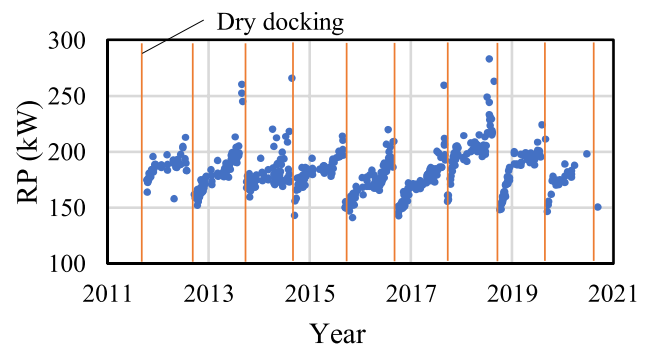


Fig. 3 Change in RP from 2011 to 2020

have some impact on the value of SP in the second period. To avoid these potential risks, the data when the rudder is at the midship position were extracted. The average of RP was calculated on each voyage and recorded as a representative value, respectively.

While a propeller is operating, the frictional forces acting between the fluid and propeller may remove fouling on the propeller. RP may have decreased during the voyage for this reason. Since the amount of decrease in fouling on a propeller may vary depending on a variety of factors, including ship speed, propeller speed, and voyage time, it is not possible to estimate the amount of change in RP during the voyage. Therefore, assuming that the variation in RP during the voyage is sufficiently small, this study used RP measured just before starting a voyage as a representative value for each voyage for the subsequent analysis.

3.3 Trend of RP

Long-term observations were implemented to trace the trend of RP. Fig. 3 shows the data of RP for the decade from September 2011 to September 2020. The orange lines indicate the timing that the ship docked in. Ship A used to go to the dock every summer season and to have a service for removing fouling from its hull and propeller. Fig. 4 shows the trend of the RP value for one year after leaving the dock each year. The legend in this figure shows the year the ship docked out. For example, "2011" includes the data from September 2011 to August 2012. RP at just the docking-out has similar values of approximately 150 kW each year. It increased by approximately 30% to 50% every year over time after leaving the dock. In addition, observing these trends closely, it is obvious that RP is increased in the period of 0–90 days since the ship left the dock. Furthermore, it peaked in the remaining period after 270 days. These periods coincide with the summer season. In general, aquatic species such as barnacles reproduce while seawater temperature is warm. In Japan, several studies have shown that some species of

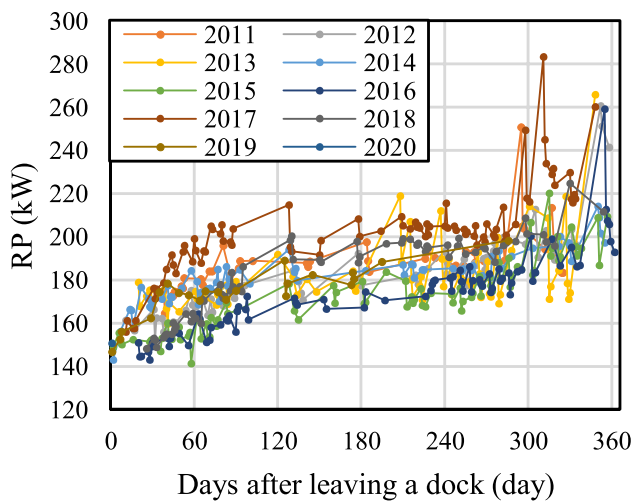


Fig. 4 Comparison between RP and elapsed days since ship A left a dock

barnacles grow at seawater temperatures of approximately 20–30°C [31–33]. The sea water temperature in Tokyo Bay is above 20°C from late May to mid-October [34]. Thus, the propeller fouled while the seawater temperature was high, which made RP larger owing to the increase in frictional loss on the propeller's surface. Additionally, in the previous studies [13, 35], steel plates were exposed to seawater for one year, and the amount of fouling attaching to the plates was observed. The weights of the fouling material on the plates increased during the summer season from May to November. In contrast, the weights increased slightly during the season when seawater temperature was low. These trends are similar to the increase in RP in this study, as shown in Fig. 4. Therefore, one may say that RP is increased by biofouling on the propeller, and the value of RP can be considered as an indicator of the propeller fouling.

In addition to biofouling, another factor that may affect the RP is the deterioration of the shaft bearing and propeller. Fig. 5 shows the median values of a whole year of RP and the RP values which can be observed for the first time after leaving the dock. The median values for each year, as well as the values immediately after docking, showed some variations. However, no apparent trend has been observed over the decade. Hence, the influence of deterioration was not considered in this study.

4 Correlation between SP and RP

4.1 Filtering and extracting data

To clarify the correlation between power for keeping propeller's rotation (RP) and the fouling, big data acquired in

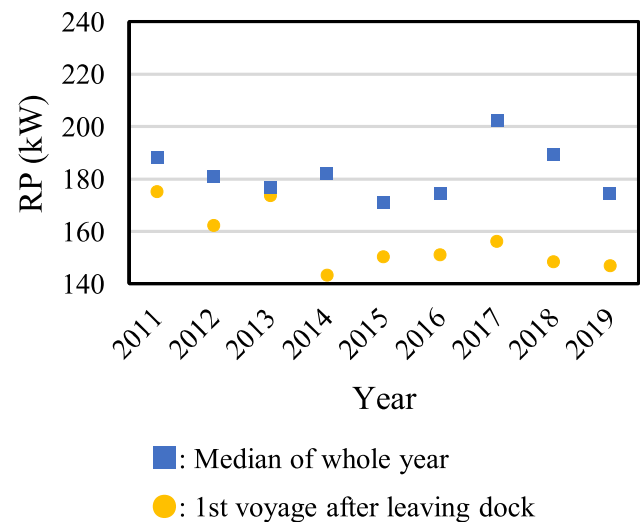


Fig. 5 Median values and values at 1st voyage after leaving a dock each year

long-term observation was analyzed. It was necessary to remove variations in data that were caused by the environmental condition and the navigation state so that static data were extracted out of the big observed one. Several filters were developed:

- 1) Filters for obtaining stable navigation data,
- 2) Filters for variations caused by environmental conditions, and
- 3) Filters for the influence of displacement.

After applying these filters, data from several operating conditions were selected to analyze the change in propulsive performance due to fouling.

4.1.1 Filters for obtaining stable navigation data

When the ship is accelerating, the propeller requires a larger power than the state with a constant ship speed. Changing the heading course affects SP even if the propeller speed and propeller blade angle are constant. Fig. 6 shows a sample of the observed data relating to the ship speed and SP on a certain day. Blue round dots are observed SP in a single-day voyage. As is clear from this figure, SP has a large variation because the ship is accelerating and changing its heading course, although the locus is expected to follow a single line if only steady-state data are collected, generally.

To figure out a correlation between SP and RP from the observed data, the filter was applied to eliminate variations in the ship speed, shaft power, shaft speed, propeller blade angle, and rudder angle [36]. The coefficient of variation (CV) filter was implemented as following schemes:

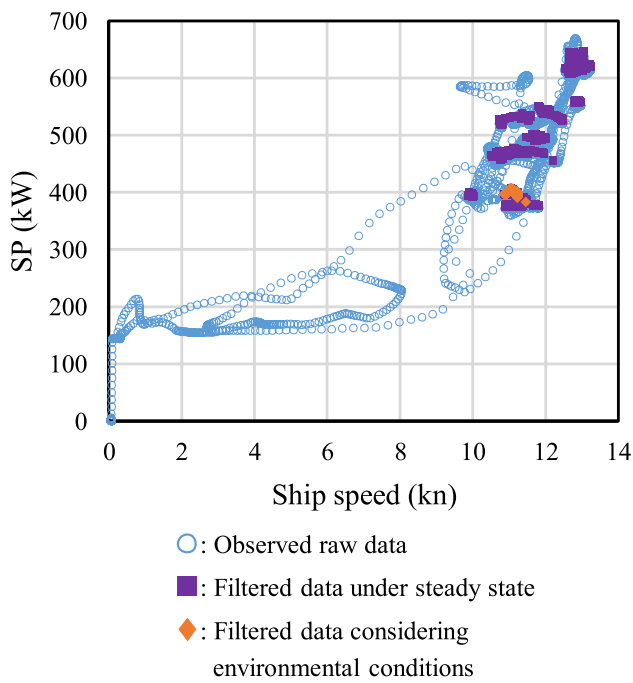


Fig. 6 Comparison of power-speed performance between observed raw data and filtered data

1. Averaging these values for a set period respectively,
2. Choosing data that satisfied the threshold values,
3. CV was calculated from the chosen data. CV was used as the threshold value to extract data that could be regarded as a quasi-steady state.

All of these schemes were applied to the observed data including ship speed, shaft power, shaft speed, propeller blade angle, and rudder angle. The extracted data were served for statistical analysis. The purple dots indicated in Fig. 6 represent the extracted data in the quasi-steady state.

4.1.2 Filters for variations caused by environmental conditions

To exclude the influence of sea and weather conditions from the data to be used for statistical analysis, environmental data that were observed in the monitoring system of the ship were utilized. Observed data relating to wind and waves are useful for assessing environmental conditions. Wind speed and direction were logged on the monitoring system, but there were no recorded data relating to waves, such as wave height, direction, and frequency. Beaufort scale (BF) was used to assess the environmental conditions for estimating the influence of waves. This value was calculated based on the observed wind speed (shown in Table 2). ISO19030-1 [37] recommends that the data can be regarded as calm sea conditions with Beaufort scale, which is less than BF 4

Table 2 Beaufort scale (Excerpt from [38])

Beaufort number	Description	Wind speed (m/s)	Probable Wave height (m)
0	Calm	0–0.2	–
1	Light air	0.3–1.5	0.1
2	Light breeze	1.6–3.3	0.2
3	Gentle breeze	3.4–5.4	0.6
4	Moderate breeze	5.5–7.9	1

(wind speed 7.9 m/s). In this study, to severely filter the data on rough sea conditions, the data set under BF 3 or less (wind speed 5.4 m/s or less) was extracted. The orange dots in Fig. 6 show the results that satisfy BF 3 or less. In this sample, less than 200 points of data were extracted from over 20,000 points of data to analyze the relationship between ship speed and SP.

4.1.3 Filters and correction for the influence of displacement

The draught of a ship changes with a displacement. If the draught increases, the area of the wetted hull surface also increases, which leads to the high resistance of the hull. To filter the influence of the displacement change, some studies that analyzed the monitoring data of a cargo ship extracted the data within small changes in draught from the reference values, such as full load condition or ballast condition. Investigating the draught based on the logbook of ship A, which this paper focuses on, the change in displacement is extremely smaller than these cargo ships because ship A is a research ship. All observed data were considered to be under the trial condition because the draught of all data were within 15 cm of the trial condition. Therefore, the data were not eliminated owing to the draught level.

Additionally, the influence of displacement was modified based on the admiralty coefficient which defines the relationship between ship speed, shaft power, and displacement [39] as follows:

$$C_{adm} = \frac{\nabla^{\frac{2}{3}} V_s^3}{SP}, \tag{1}$$

where C_{adm} is the admiralty coefficient; ∇ is displacement; V_s is ship speed; SP is shaft power.

Each vessel has an eigenvalue of the admiralty coefficient. From Eq. 1, if a vessel navigates at a constant ship speed, displacement and shaft power satisfy the following relationship:

$$C_{adm} = \frac{\nabla^{\frac{2}{3}} V_s^3}{SP} = \frac{\nabla_{(trial)}^{\frac{2}{3}} V_s^3}{SP_{(trial)}} \tag{2}$$

$$SP_{(trial)} = SP \times \left(\frac{\nabla_{(trial)}}{\nabla} \right)^{\frac{2}{3}} \tag{3}$$

where $\nabla_{(trial)}$ is displacement at the trial condition; ∇ is displacement of the observed data; $SP_{(trial)}$ is shaft power at the trial condition; SP is observed shaft power.

The shaft power under the trial condition ($SP_{(trial)}$) can be estimated based on Eq. 3. In this analysis, the displacement on each day was estimated from the value of draught, and the change in shaft power affected by displacement was corrected using the admiralty coefficient. This modification corrected the shaft power by up to 5%.

4.1.4 Operating conditions

Generally, ship officers determine ship speed by ordering several simple steps, such as “slow ahead”, “half ahead”, and “full ahead”. Therefore, it is important to focus on these specific conditions for statistical analysis. This paper chose three conditions with a blade angle of 9.3 deg., 13.4 deg., and 17.3 deg. (within ± 0.2 deg.)

The median values of SP at each operating condition were calculated from the extracted data on each voyage and regarded as a representative value of each voyage.

4.2 The correlation between SP and RP

By implementing the filters mentioned above, quasi-steady-state data were extracted from the big data and the correlation between RP and SP was analyzed. In Fig. 7, the data

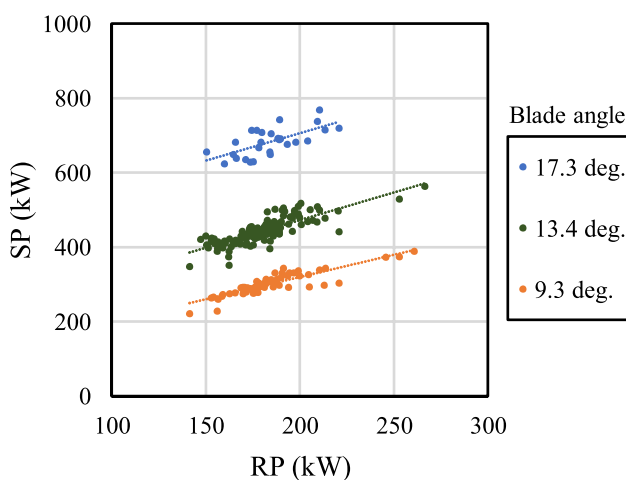


Fig. 7 Correlation between SP and RP at three operating conditions

at three operating conditions are color-coded. Additionally, regression lines at each condition were obtained using the linear least squares method. Assuming a linear correlation between SP and RP , the following regression model is suggested:

$$SP = a \cdot RP + b \tag{4}$$

where a and b are the coefficients of regression. The coefficients were determined using the linear least squares method, and these are presented in Table 3. The regression lines for each operating condition are shown in Fig. 7. From a statistical viewpoint, RP and SP have a linear positive correlation, regardless of the propeller blade angle.

If the value of slope “ a ” is 1.0, the increase in RP is equal to the increase in SP . This means that the change in SP is affected only by the propeller fouling because it is considered that the value of RP is influenced by the propeller fouling as we discussed in Chapter 3. However, the values of “ a ” were greater than 1.0. The increase in SP was larger than that in RP . Thus, it is considered that SP is influenced not only by the propeller fouling but also by the change in hull resistance due to the hull fouling. In addition, the increase in SP was proportional to the increase in RP . Consequently, one may assume that the value of RP can be regarded as an index showing not only the propeller fouling, but hull fouling.

4.3 Change in power-speed performance due to biofouling

Fouling on the surface of the hull and propeller increases the frictional resistance, which leads to an increase in the shaft power. To simplify the influence of fouling on the shaft power, the observed data were classified into three groups based on the value of RP , as follows.

1. Clean condition: $RP = 150 \pm 5kW$
2. Fouled slightly condition: $RP = 180 \pm 5kW$
3. Fouled seriously condition: $RP = 210 \pm 5kW$

Data with RP values within ± 5 kW from the values of the above conditions were extracted from the observed data to conform to each condition. Furthermore, as shown in Fig. 8, the data were grouped into three by the blade

Table 3 Coefficient values expressing correlation between SP and RP

Operating Condition	Number of samples	a	b
17.3 deg.	27	1.482	410.83
13.4 deg.	134	1.485	176.57
9.3 deg.	61	1.190	82.18

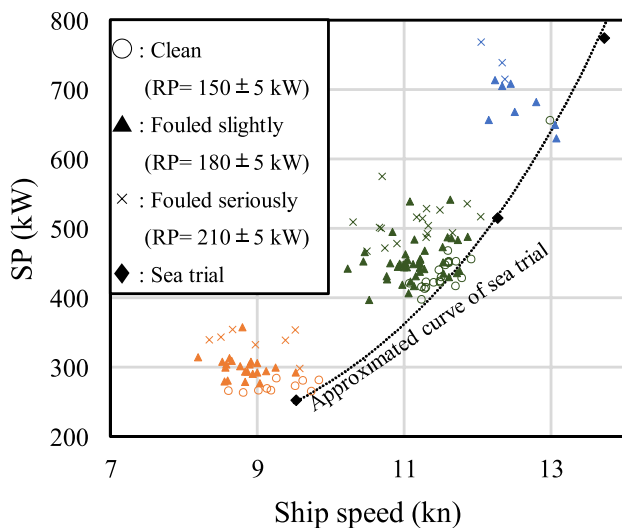


Fig. 8 Comparison of power-speed performance with data from clean condition, two fouled conditions, and sea trial

angle with the same colors as in Fig. 7. The blue plots states operating at 17.3 deg. of the CPP, green color indicates 13.4 deg., and orange one indicates 9.3 deg., respectively. For instance, the green cross mark shows SP under the following conditions:

- (1) The state is fouled seriously,
- (2) The propeller blade angle is 13.4 ± 0.2 deg., and
- (3) The data are at the steady state and not significantly affected by environmental factors.

Additionally, Fig. 8 shows the approximated curve of the performance during the sea trial which was conducted just before the delivery of ship A. The data from the sea trial shows an initial performance because the hull and propeller were clean and new, and the weather conditions were calm at that time.

Ship A was built in 1987. Therefore, this ship was already an old vessel when this monitoring and logging began in 2010. Hence, it was concerned about the influence of aging degradation. Comparing the extracted data to the approximated curve at the sea trial, the data in the clean condition, which is shown in the circle plot, indicates that the performance is close to that of the sea trial. It means that the propulsion performance did not suffer aging degradation significantly. The ship speed decreased by more than 1 knot at a constant shaft power compared to the performance curve at sea trial. The shaft power was increased by more than 100 kW at constant ship speed as well. In the worst case, shaft power was raised by 50% from the sea trial level. As a result, data on voyages with high RP show a decrease in ship speed and an increase in the shaft power compared with data on voyages with low RP. Therefore, the assumption that the

fouling progress could be estimated from the change in RP was proven.

5 Biofouling influence on shaft power

As shown in Section 4.3, biofouling has an impact of increasing shaft power and decreasing ship speed. This section focuses only on the changes in shaft power under several fouling conditions. To clarify the correlation between the change in shaft power and fouling condition, it is necessary to compare the value of shaft power at a constant speed between clean and fouled conditions. For this reason, it was attempted to formulate the relationships between ship speed and shaft power under each condition and fit the power-speed curves using Ordinary Least Squares (OLS).

5.1 Pre-processing of analysis data

In Chapter 4, several filters were implemented to reduce the scattered data caused by environmental conditions and the navigation state. To extract purified data from the observed data, additional filters were implemented for eliminating the scattered data due to the error of the speed measurements in Section 5.1.1 and the disturbance by wind in Section 5.1.2.

Additionally, the analysis data were concentrated within a narrow range of ship speeds. To estimate the power-speed curves with good accuracy, the correction for imbalanced data in terms of the number of data was performed using the oversampling technique in Section 5.1.3.

5.1.1 Filter for log speed error

Vessels have two types of ship speed: speed through the water (Log speed) and speed over the ground (OG speed). Generally, the propulsive performance of a vessel is evaluated using the log speed. On the other hand, a log speed measuring device often has errors due to fouling on the sensor and floating matters underwater. The following equation was used as an additional criterion to clean the data complying with ISO19030-1 [37]:

$$|v_l - v_g| \leq 0.2, \quad (5)$$

where v_l is Log speed in knot; v_g is OG speed in knot.

5.1.2 Correcting the change in power due to wind resistance

Wind disturbance was estimated based on the observed wind speed and wind direction. The correction method for wind resistance was based on ISO19030-2 [36], as shown below:

$$SP_{\text{corr}} = SP - \Delta P_W, \tag{6}$$

$$\Delta P_W = \frac{(R_{\text{rw}} - R_{0w}) \cdot v_g}{\eta_D \eta_H \eta_R \eta_M}, \tag{7}$$

$$R_{\text{rw}} = \frac{1}{2} \cdot \rho_a \cdot v_{\text{wr}}^2 \cdot A \cdot C_{\text{rw}}(\psi_{\text{wr_ref}}), \tag{8}$$

$$R_{0w} = \frac{1}{2} \cdot \rho_a \cdot v_g^2 \cdot A \cdot C_{0w}(0), \tag{9}$$

where SP_{corr} is the corrected shaft power in W; ΔP_W is the increase in shaft power due to wind in W; R_{rw} is the wind resistance due to relative wind in N; R_{0w} is the air resistance in no-wind condition in N; v_g is the ship speed over ground in m/s; v_{wr} is the relative wind speed at reference height in m/s; $\psi_{\text{wr_ref}}$ is the wind direction of relative wind; C_{rw} is the wind resistance coefficient depending on $\psi_{\text{wr_ref}}$; C_{0w} is the wind resistance coefficient for head wind (0° wind direction); ρ_a is the air density in kg/m^3 ; A is the transverse projected area in current loading condition in m^2 ; η_O is the open-water efficiency of the propeller; η_H is the hull efficiency; η_R is the relative rotative efficiency; η_M is the mechanical efficiency considering the mechanical loss of the shaft bearing.

RIOS [40] was used as a platform to calculate the wind resistance coefficient based on Fujiwara’s method [41]. The transverse projected area, the relative rotative coefficient, and the hull coefficient of ship A were referenced from the design documents of ship A. In addition, the open-water efficiency of the propeller was estimated from the design diagrams of the AU-CP propeller [42].

5.1.3 Correction for imbalanced data

Figure 9 shows the distributions of the data on ship A versus the rounded ship speed. Ship A often navigated at the full ahead state which realized around 11 knots. Therefore, 50–70% of all the data exist at approximately 11 knots at each fouled condition. From this result, the dataset had an uneven distribution in terms of ship speed. To figure a proper approximated curve out of the filtered data, an imbalanced distribution of data may lead to an over-fitting issue. In this case, this dataset may cause over-fitting, which brings good accuracy around 11 knots, whereas fitting curves may not match the observed other speed range. To avoid over-fitting, the dataset was classified into four groups as shaft power, and Synthetic Minority Oversampling Technique (SMOTE) was used to equalize the number of data in each group. Table 4 lists the classification conditions used in this study. It shows the number of data points before and after the oversampling for each condition. Additionally, considering the error rate of the sensors and measurement devices

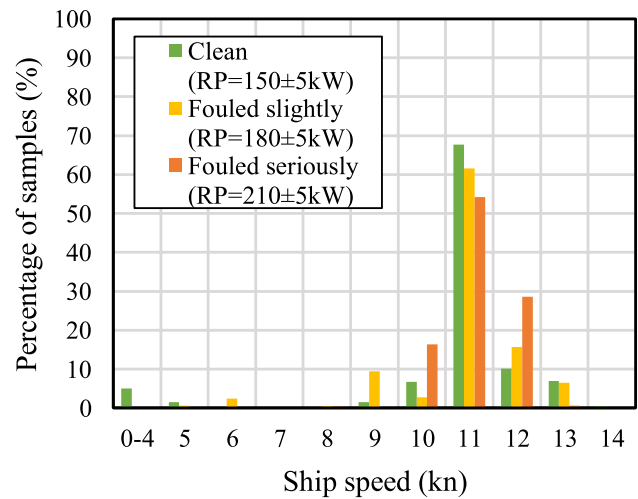


Fig. 9 Distribution of ship speed in observed data

Table 4 Classification for oversampling in the clean condition ($RP = 150 \pm 5 \text{ kW}$)

Label	SP (kW)	Number of original data	Number of data after compensation
0	<250	46	368
1	250–350	197	368
2	350–550	368	368
3	550<	49	368

at low speed, data under 8 knots were excluded from the analysis data [37]. After these pre-processing steps were implemented, the correlation between the shaft power and the ship speed was formulated, and the power-speed performance curves were estimated.

5.2 Estimation of power-speed performance curve

Performance curves of each fouling condition were estimated using the OLS method. The regression model between the ship speed and SP suggested by ITTC [43] is as follows:

$$SP = a \cdot v_1^b + c, \tag{10}$$

where a , b , and c are the coefficients of regression; v_1 is log speed in knot; SP is shaft power in kW. Unknown constant " c " is the intercept of the performance curve. In the case of a ship equipped with a fixed pitch propeller (FPP), the propeller does not require power while the ship speed is zero because the FPP is not rotating. Hence, intercept " c " is often set to zero as specified in ISO19030-3 [44]. However,

as described in Section 3, a CPP requires power to some extent even if the ship speed is zero, because it is driven at its rated speed in seawater even if the net thrust force is zero. It is considered that SP equals RP at $v_1 = 0$ knot. Thus, RP can be substituted as the intercept "c" for (10). Therefore, Eq. 10 can be expressed as follows:

$$SP = a \cdot v_1^b + RP, \tag{11}$$

where RP is a constant value determined for each fouling condition in kW. To use the linear least squares method, the model is linearized by taking the logarithms of both sides as:

$$\log(SP - RP) = \log a + b \log v_1. \tag{12}$$

The coefficients were determined using the linear least squares method, and are presented in Table 5. To evaluate the accuracy of estimated curves, R^2 coefficients were calculated using the following formula:

$$R^2 = 1 - \frac{\sum (y - \hat{y})^2}{\sum (y - \bar{y})^2}, \tag{13}$$

where R^2 is a coefficient of determination; y is an observed value before oversampling; \hat{y} is an estimated value based on the linear least squares method; \bar{y} is an arithmetic mean of observed value. Table 5 shows that R^2 values are over 0.8 in every conditions. This result indicates that the regression models have good accuracy. In addition, the performance curves were drawn based on the coefficients, as shown in Fig. 10.

5.3 Power increasing ratio due to the propeller fouling

From the estimated curves, the changes in shaft power at constant speed were calculated in the interpolated interval between ship speeds of 8 and 12 knots. Fig. 11 shows the required shaft power to maintain a constant speed at each fouling condition. The results indicated that SP was increased as fouling progressed under all ship speed conditions. SP was increased by 20% on average in a slightly fouled condition ($RP = 180$ kW) and by 35% on average in a serious fouled condition ($RP = 210$ kW) compared to SP in a clean condition ($RP = 150$ kW), respectively. In addition,

Table 5 Coefficient values expressing regression models

Condition	Number of Samples	a	b	c	R^2
Clean	1104	0.010	4.199	150	0.980
Fouled slightly	8968	0.036	3.728	180	0.851
Fouled seriously	1512	0.018	4.098	210	0.839

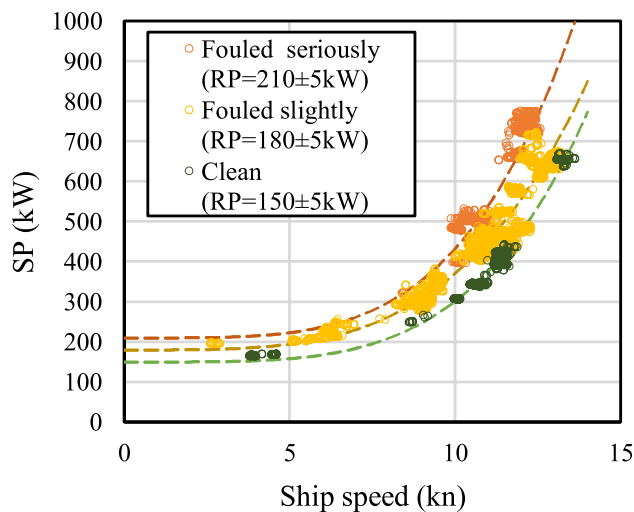


Fig. 10 Comparison between power–speed estimated curves and observed raw data

the increase in power owing to fouling can be achieved by the following calculation:

$$\Delta SP = SP_{\text{fouled}} - SP_{\text{clean}}, \tag{14}$$

$$\Delta RP = RP_{\text{fouled}} - RP_{\text{clean}}, \tag{15}$$

where ΔSP is the change in shaft power (SP) in kW; ΔRP is the change in power for keeping propeller’s rotation (RP) in kW. Fig. 12 shows the correlation between ΔSP and ΔRP under the two fouled conditions. This study assumed that ΔRP was caused by fouling on the propeller. Fouling on the propeller affects the propulsion performance not only in the RP state with a neutral blade angle but also during normal navigation. Hence, ΔSP has to include ΔRP . If the data are on a linear line with a slope 1, ΔSP can be attributed only to

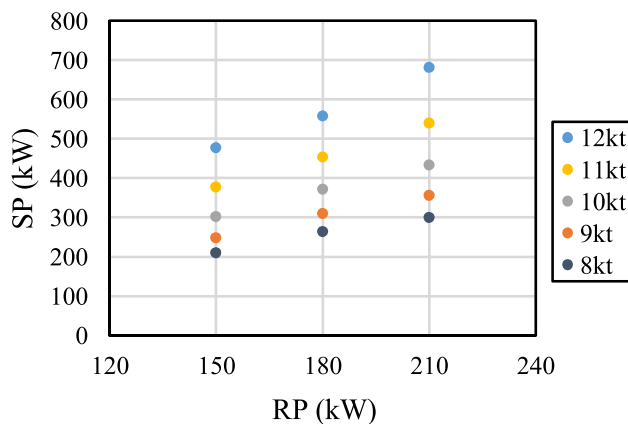


Fig. 11 SP and RP at five estimated points of ship speed

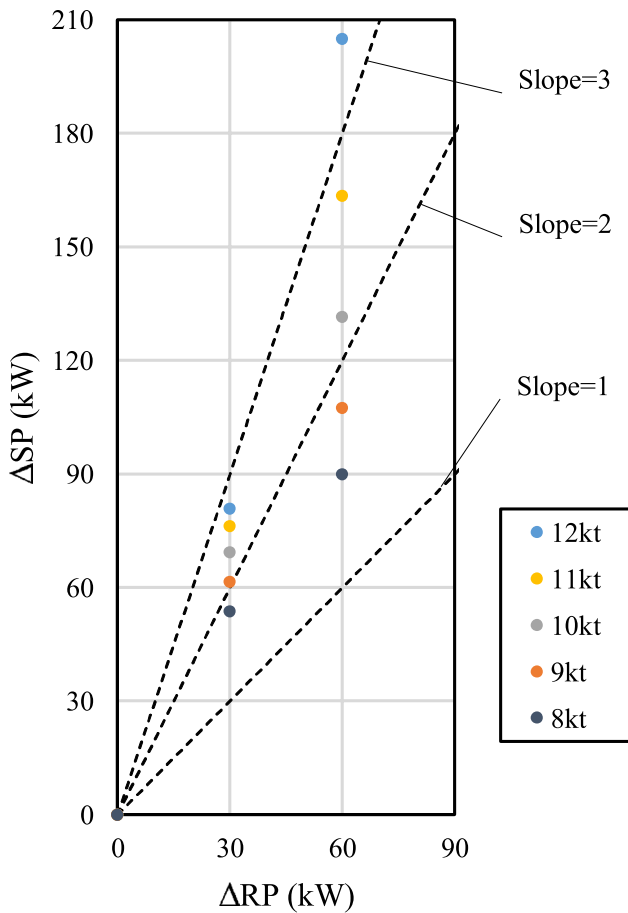


Fig. 12 Correlation of increase in power between SP and RP

the propeller fouling. However, all plotted data are above the line with a slope of 1. It means that ΔSP consists of ΔRP and an increase of the other in SP . Another factor that led to an increase in SP is assumed to be the hull fouling. The breakdown of ΔSP can be expressed using the following equation:

$$\Delta SP = \Delta RP + \Delta P_{\text{other}} \tag{16}$$

where ΔP_{other} is the increase in shaft power due to another factors other than the propeller fouling in kW. Fig. 13 visualizes the breakdown of ΔRP and ΔP_{other} in a bar chart. The entire bar shows ΔSP . Figs. 12 and 13 indicate that ΔRP occupied over one-third of ΔSP below 11 knots. In addition, ΔRP occupied slightly more than half of ΔSP below 9 knots. As the results, the ratio of ΔSP due to the propeller fouling is changed with ship speed, and when the ship speed is lower, the influence of propeller fouling tends to have a large impact in ΔSP .

The rotational speed of the propeller blade is faster than its advanced speed. It is thought that the increase in shaft power caused by the fouling on the propeller is strongly

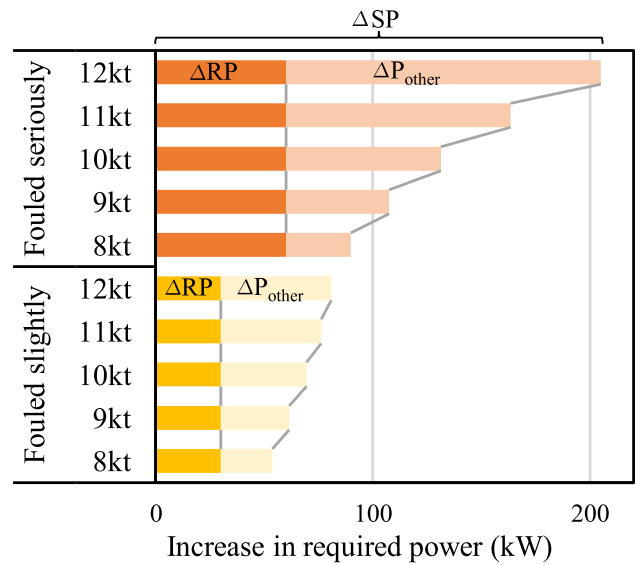


Fig. 13 Comparison between ΔRP and ΔP_{other} as a percentage of ΔSP

influenced by not the propeller’s advanced speed which is approximately proportional to the ship speed but the propeller’s rotational speed. CPP is driven at a constant speed under all ship speed conditions. Thus, RP and ΔRP can be regarded as constants. On the other hand, it is thought that the increase in shaft power caused by fouling on the hull is sensitive to the ship speed. From these considerations, as is clear from Fig. 13, the propeller fouling has an impact on the increase in shaft power when the ship speed is low, especially. In the cases of the coastal liners with CPP, such as ship A, they often navigate at low ship speeds, and the CPP is driven at its rated speed. Therefore, the shaft power and ship speed are significantly affected by fouling on the propeller.

6 Conclusion

In this study, the influence of fouling was analyzed based on the observed data on an actual ship. This study focused on shaft power (SP) at the neutral blade angle of a CPP to observe the increase in SP due to fouling on the propeller. This power was defined as the power for keeping propeller’s rotation (RP) in this paper. In the case of the investigated ship A, RP was increased from 30 to 50% after leaving a dock for a year. Specifically, RP was raised significantly when sea temperature was high in the summer season. The fouling influence affecting the ship speed and SP was analyzed by extracting quasi-steady data from the observed data. The observed data from a voyage with a high value of RP showed a decrease in ship speed and an increase in shaft power at the same driven conditions. Considering these

results, one may conclude that the change in RP indicates the state of fouling on the propeller and hull.

To analyze the increases in SP and RP under the same fouling conditions, the required shaft power to navigate at a constant speed was estimated, and the fouling on the ship was classified into three conditions based on the values of RP. The influence of fouling on the required shaft power is affected by the ship speed. In the case of ship A, which has a CPP, fouling on the hull has a larger influence than the propeller fouling when the ship navigates at high speed. However, when the ship runs at low speed, the fouling on the propeller has a more serious impact to increase the shaft power than the hull fouling.

Data availability The raw data had been generated on ship A. The authors have no right to redistribute the data.

Open Access This article is licensed under a Creative Commons Attribution 4.0 International License, which permits use, sharing, adaptation, distribution and reproduction in any medium or format, as long as you give appropriate credit to the original author(s) and the source, provide a link to the Creative Commons licence, and indicate if changes were made. The images or other third party material in this article are included in the article's Creative Commons licence, unless indicated otherwise in a credit line to the material. If material is not included in the article's Creative Commons licence and your intended use is not permitted by statutory regulation or exceeds the permitted use, you will need to obtain permission directly from the copyright holder. To view a copy of this licence, visit <http://creativecommons.org/licenses/by/4.0/>.

References

- Townsin RL (2003) The ship hull fouling penalty. *Biofouling* 19:9–15
- IMO (2022) GHG emissions. <https://www.glofouling.imo.org/ghg-emissions> Accessed 11 Dec 2021
- IMO (2021) Preliminary results: Impact of ships' biofouling on greenhouse gas emissions. <https://wwwcdn.imo.org/localresources/en/MediaCentre/Documents/Biofouling%20report.pdf>. Accessed 1 Dec 2021
- Hewitt CL, Campbell ML (2010) The relative contribution of vectors to the introduction and translocation of invasive marine species. The Department of Agriculture, Fisheries and Forestry (DAFF)
- IMO (2022) Biofouling and IAS. <https://www.glofouling.imo.org/the-issue> Accessed 3 Mar 2022
- Schultz MP (2011) Economic impact of biofouling on a naval surface ship. *Biofouling* 27(1):87–98
- MEPC62 (2011) Amendments to the annex of the protocol of 1997 to amend the international convention for the prevention of pollution from ships, 1973, as modified by the protocol of 1978 relating thereto. pp 1–25
- MEPC72 (2018) Initial IMO strategy on reduction of GHG emissions from ships. pp 1–10
- MEPC70 (2016) 2016 guidelines for the development of a ship energy efficiency management plan (SEEMP). pp 1–15
- Hiraga Y (1934) Experimental investigations on the frictional resistance of planks and ship-models. *J Zosen Kiokai* 1934(55):101–158
- Hiraga Y (1934) Experimental investigations on the resistance of long planks and ships. *J Zosen Kiokai* 1934(55):159–199
- Taylor DW (1910) *The speed and power of ships*, vol 2. Wiley, New York
- McEntee W (1915) Variation of frictional resistance of ships with condition of wetted surface. *Transact Soc Naval Architects Marine Eng* 23:37–42
- McEntee W (1916) Notes from model basin. *Transact Soc Naval Architects Marine Eng* 24:85–89
- Song S, Demirel YK, Atlar M (2019) An investigation into the effect of biofouling on full-scale propeller performance using CFD. In: *Proceedings of the ASME 2019 38th International Conference on Offshore Mechanics and Arctic Engineering*, Glasgow, Scotland, UK
- Granville PS (1958) The frictional resistance and turbulent boundary layer of rough surfaces. *J Ship Res* 2(04):52–74
- Seo KC, Altar M, Goo B (2016) A study on the hydrodynamic effect of biofouling on marine propeller. *J Korean Soc Marine Environ Safety* 22(1):123–128
- Schultz MP (2007) Effects of coating roughness and biofouling on ship resistance and powering. *Biofouling* 23(5):331–341
- Demirel YK, Turan O, Incecik A (2017) Predicting the effect of biofouling on ship resistance using CFD. *Appl Ocean Res* 62:100–118
- Song S, Dai S, Demirel YK et al (2021) Experimental and theoretical study of the effect of hull roughness on ship resistance. *J Ship Res* 65(01):62–71
- Song S, Demirel YK, Muscat-Fenech CDM et al (2020) Fouling effect on the resistance of different ship types. *Ocean Eng* 216(107):736
- Farkas A, Degiuli N, Martić I et al (2020) Performance prediction method for fouled surfaces. *Appl Ocean Res* 99(102):151
- Farkas A, Degiuli N, Martić I (2021) Assessment of the effect of biofilm on the ship hydrodynamic performance by performance prediction method. *Int J Naval Architecture Ocean Eng* 13:102–114
- Song S, Demirel YK, Atlar M (2020) Penalty of hull and propeller fouling on ship self-propulsion performance. *Appl Ocean Res* 94(102):006
- Izubuchi T (1934) Experimental investigations on the resistance of long planks and ships. *J Zosen Kiokai* 1934(55):57–100 ((In Japanese))
- Coraddu A, Lim S, Oneto L et al (2019) A novelty detection approach to diagnosing hull and propeller fouling. *Ocean Eng* 176:65–73
- Coraddu A, Oneto L, Bald F et al (2019) Data-driven ship digital twin for estimating the speed loss caused by the marine fouling. *Ocean Eng* 186(106):063
- Carchen A, Atlar M, Turkmen S et al (2019) Ship performance monitoring dedicated to biofouling analysis: Development on a small size research catamaran. *Appl Ocean Res* 89:224–236
- Carchen A, Atlar M (2020) Four KPIs for the assessment of biofouling effect on ship performance. *Ocean Eng* 217(107):971
- van Manen JD (1973) Non-conventional propulsion devices. *Int Shipbuild Prog* 20(226):173–193
- Hanabusa M (1999) Research of adhered tendency of sessile organisms about interrelation between material of experiment plates and amount of sessile organisms : An experiment at the inner part of ORIDO bay. *Navigation* 142:47–53 ((In Japanese))
- Yasuda T (1970) Ecological studies on the marine fouling organisms occurring along the coast of Fukui prefecture. *Nippon Suisan Gakkaishi* 36:1007–1016 ((In Japanese))
- Iwaki T (1981) Reproductive ecology of some common species of barnacles in japan. *Marine fouling* 3(1):61–69 ((In Japanese))
- Yauchi E (2019) Reasons for the absence of green tides in inner Tokyo bay in 2017–2018. *Journal of Japan Society of Civil*

- Engineers Ser B2 (Coastal Engineering) 75(2):I_1069–I_1074. (In Japanese)
35. Saito T (1931) Researches in fouling organisms of the ship's bottom. Zosen Kiokai Kaihou pp 13–64. In Japanese
 36. ISO (2016a) ISO19030-2, ship and marine technology - measurement of changes in hull and propeller performance - part 2: default method, Annex G Correction for wind resistance. pp 25–26
 37. ISO (2016b) ISO19030-1, ship and marine technology - measurement of changes in hull and propeller performance - part 1: general principles, Annex A Method and assumptions for estimating the uncertainty of a performance analyses process. pp 13–19
 38. WMO (2019) Manual on codes - international codes, volume I.1, annex II to the wmo technical regulations, part a - alphanumeric codes, Section E Beaufort scale of wind. p 379
 39. Sakurada A, Sogihara N, Tsujimoto M (2020) Development of a filtering method for evaluation of performance in a calm sea based on onboard monitoring data. J Jpn Soc Naval Architects Ocean Eng 31:29–37
 40. RIOS (2020), Research Initiative on Oceangoing Ships, Department of Naval Architecture and Ocean Engineering, Division of Global Architecture, Graduate School of Engineering, Osaka University, <http://www.rios.eng.osaka-u.ac.jp/>. Accessed 20 Jul 2020
 41. Fujiwara T, Ueno M, Ikeda Y (2005) A new estimation method of wind forces and moments acting on ships on the basis of physical component models. J Jpn Soc Naval Architects Ocean Eng 2:243–255
 42. Yazaki A, Kuramochi E, Osaki T (1962) Design diagrams of four-bladed controllable pitch propellers. J Zosen Kiokai 112:73–83
 43. ITTC (2021) Recommended procedures and guidelines, 7.5-04-01- 01.1 preparation, conduct and analysis of speed/power trials. pp 61–63
 44. ISO (2016) ISO19030-3, ship and marine technology - measurement of changes in hull and propeller performance - part 3: Alternative methods, 5.4.2.3.5 Fitting speed-power curve to obtained data. pp 8–9

Publisher's Note Springer Nature remains neutral with regard to jurisdictional claims in published maps and institutional affiliations.